Journal of Hazardous Materials 164 (2009) 838–846

Contents lists available at ScienceDirect

Journal of Hazardous Materials

journal homepage: www.elsevier.com/locate/jhazmat

Gas–liquid hybrid discharge-induced degradation of diuron in aqueous solution

Jingwei Feng, Zheng Zheng*, Jingfei Luan, Kunquan Li, Lianhong Wang, Jianfang Feng

State Key Laboratory of Pollution Control and Resource Reuse, School of the Environment, Nanjing University, Nanjing 210093, PR China

ARTICLE INFO

Article history:
Received 16 February 2008
Received in revised form 14 June 2008
Accepted 25 August 2008
Available online 30 August 2008

Keywords:
Diuron
Gas–liquid hybrid discharge
Degradation efficiency
Degradation pathway

ABSTRACT

Degradation of diuron in aqueous solution by gas–liquid hybrid discharge was investigated for the first time. The effect of output power intensity, pH value, Fe^{2+} concentration, Cu^{2+} concentration, initial conductivity and air flow rate on the degradation efficiency of diuron was examined. The results showed that the degradation efficiency of diuron increased with increasing output power intensity and increased with decreasing pH values. In the presence of Fe^{2+}, the degradation efficiency of diuron increased with increasing Fe^{2+} concentration. The degradation efficiency of diuron was decreased during the first 4 min and increased during the last 10 min with adding of Cu^{2+}. Decreasing the initial conductivity and increasing the air flow rate were favorable for the degradation of diuron. Degradation of diuron by gas–liquid hybrid discharge fitted first-order kinetics. The pH value of the solution decreased during the reaction process. Total organic carbon removal rate increased in the presence of Fe^{2+} or Cu^{2+}. The generated Cl^{-1}, NH_4^+, NO_3^-, oxalic acid, acetic acid and formic acid during the degradation process were also detected. Based on the detected Cl^{-1} and other intermediates, a possible degradation pathway of diuron was proposed.

1. Introduction

Diuron is a non-selective herbicide, which is mainly used for weed eradication. Diuron is highly persistent (one month to one year) in the environment [1] and the wide use of diuron in agriculture has led to pollution of the environment. Diuron's potential to pollute water is of particular concern. Diuron may contaminate the surface water by agricultural runoffs and wastewaters generated from diuron manufacturing plants [2]. In Japan, The Netherlands and United Kingdom, diuron is usually detected in the aquatic environment [3–5]. Furthermore, diuron is a considered priority substance by the European Union Water Framework Directive (Directive 2000/60/EC) [6]. Several advanced oxidation processes (AOPs) such as electrochemical method, photocatalytic oxidation, photo-Fenton and photocatalytic ozonation have been investigated for diuron degradation [7–14].

Recently, another advanced oxidation process called gas–liquid hybrid discharge has attracted the attention of many researchers for the application of pollutant degradation in aqueous solution. In gas–liquid hybrid discharge process, energy is injected into the aqueous solution through the plasma channel formed by pulsed high-voltage discharge between electrodes [15]. Gas–liquid hybrid discharge is demonstrated to initiate a variety of physical and chemical effects in water including UV radiation, shock waves and the formation of various active species such as radicals ($HO^•$, $O^•$, $H^•$) and molecular specials (H_2O_2, O_3) [16–22]. Thus, the degradation of 4-chlorophenol [15,23], dye [24] and phenol [25] was performed by gas–liquid hybrid discharge. While the degradation of diuron in aqueous solution by gas–liquid hybrid discharge has not been reported in the literature. Therefore, the purpose of the present work is to investigate the degradation behavior and degradation mechanism of diuron in aqueous solution by gas–liquid hybrid discharge. At the same time, several factors affecting the degradation efficiency of diuron are studied.

2. Materials and methods

2.1. Chemicals

Diuron (analytical standard, purity grade, 99.5%) was purchased from Sigma–Aldrich. Methanol used in the analysis was high-performance liquid chromatography (HPLC) grade. Other chemicals were all analytical grade and used without further purification. $FeSO_4{\cdot}7H_2O$ and $CuSO_4{\cdot}5H_2O$ were used as the source of Fe^{2+} and Cu^{2+}, respectively. Na_2SO_4 (0.1 mol L^{-1}) were used to adjust the conductivity of the solution. H_2SO_4 and NaOH were used to adjust the pH value of the solution.

2.2. Experimental process

It is shown in Fig. 1 that the experimental apparatus consisted of a gas–liquid hybrid discharge reactor and a pulsed high

* Corresponding author. Tel.: +86 25 83593109; fax: +86 25 83707304.
E-mail address: zzheng@nju.edu.cn (Z. Zheng).

0304-3894/$ – see front matter © 2008 Elsevier B.V. All rights reserved.
doi:10.1016/j.jhazmat.2008.08.085

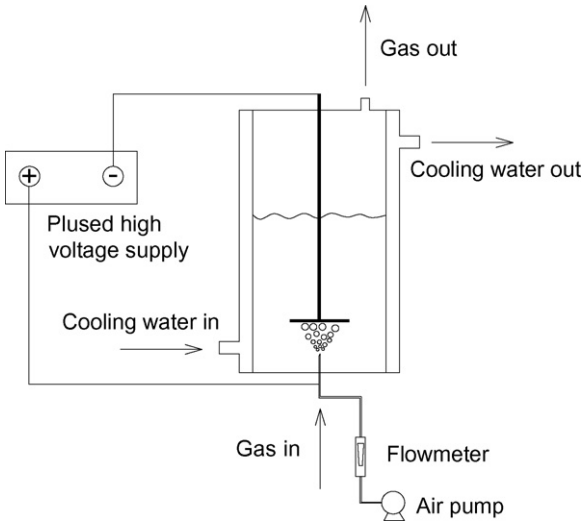

Fig. 1. Schematic diagram of the experimental apparatus.

voltage power supply. The gas–liquid hybrid discharge reactor, which contained a needle-plate electrode, was 50 mm in inner diameter and 100 mm in height. The positive electrode was a hollow stainless steel injection needle of 0.7 mm in diameter and the negative electrode was a stainless steel square of 4 cm^2 in the area. The distance between positive electrode and negative electrode was 10 mm. The air was bubbled through the needle. The gas–liquid hybrid discharge reactor was cooled by cooling water. The power was supplied by a pulsed high voltage source (Hefei Yingdong Technology Co., Ltd., China), which could be operated at an adjustable amplitude voltage. The intensity of discharge in the reactor could be denoted by the output power intensity. All samples were prepared in water purified by a Millipore Milli-Q system. For every experiment, 100 mL solution was added into the reactor. Phosphate buffered solution was used to examine the effect of pH value on the degradation efficiency of diuron.

2.3. Analysis

The concentration of diuron was analyzed by a HPLC system (Agilent, USA, 1200 Series) equipped with Hypersil ODS HPLC column (250 mm × 4.6 mm i.d., 5 μm, Agilent, USA), a multiple wavelength UV diode array detector and an auto sampler controlling under a Chemstation data acquisition system. The eluent consisted of 70% methanol and 30% water, and the flow rate was 1.0 mL min^{-1}. The column temperature was kept at 30 °C. The degradation efficiency of diuron was calculated from the following Eq. (1):

$$\eta = \left(\frac{C_0 - C_t}{C_0}\right) \times 100\% \quad (1)$$

where η was the degradation efficiency of diuron (%), C_t was the residual concentration of diuron after discharge treatment (mmol L^{-1}) and C_0 was the initial concentration of diuron before discharge treatment (mmol L^{-1}).

Total organic carbon (TOC) was determined on a Shimadzu 5000A TOC analyzer. pH value of the solution was measured by a pH monitor (Shanghai Kangyi Instrument Co., Ltd., China, PHS-2C). The conductivity of the solution was measured by a DDS-11 AW conductivity meter. Cl^- and NO_3^- were detected by ion chromatography (IC) (ICS-1000, anions column ASRS-ULTRAII, 4 mm). The eluent was NaOH (30 mmol L^{-1}) and the flow rate was 1.0 mL min^{-1}. Nesster's reagent colorimetric method was used for the determination of NH_4^+ [26]. Phenanthroline spectrophotometry was used to determine the concentration of Fe^{2+} in the solution [26]. The concentration of H_2O_2 was determined spectrophotometrically [27]. Acetic acid, formic acid and oxalic acid were also detected by ion chromatography (IC) (ICS-1000, anions column ASRS-ULTRAII, 4 mm). The eluent was KOH (0.8 mmol L^{-1}) and the flow rate was 1.0 mL min^{-1}.

The identification of diuron and its degradation products was performed by liquid chromatography–mass spectrometer (LC–MS) (ThermoQuestLCQ Duo, USA) with ZORBAX Rx-C_{18} HPLC column (150 mm × 2.1 mm i.d., 5 μm, Agilent, USA). 10 μL of solution after treatment was injected automatically into the LC–MS system. The eluent consisted of 60% methanol and 40% water, and the flow rate was 0.2 mL min^{-1}. The other LC conditions were the same as the conditions used in determining diuron concentration. MS conditions were as follows: the electrospray ionization interface was selected. The capillary temperature was set to 275 °C with a voltage of 19.00 V. The spray voltage was 5000 V and the sheath gas flow rate was 18 arb. The spectra were acquired in the negative ion scan mode, over the m/z range from 50 to 600.

3. Results and discussion

3.1. The factors affecting the degradation efficiency of diuron

3.1.1. Effect of output power intensity on the degradation efficiency of diuron

It is shown in Fig. 2 that the degradation efficiency of diuron increased with increasing output power intensity. For example, the degradation efficiency of diuron was 65.5% after 4 min of reaction time in the case of 35 W. While at the same discharge time the degradation efficiencies of diuron were 73.5 and 89.2% under the condition of 45 and 60 W, respectively. The reason was that the discharge intensity increased with increasing output power intensity which has been injected into the reactor, thus, the intensity of UV radiation and shock waves increased. Simultaneously, the amount of the active species ($HO^•$, $O^•$, $H^•$, H_2O_2, O_3) also increased with increasing output power intensity. Based on above results, the oxidation amount of diuron was increased.

In order to compare the reaction rates in the gas–liquid hybrid discharge reactor, the experimental data were fitted by the follow-

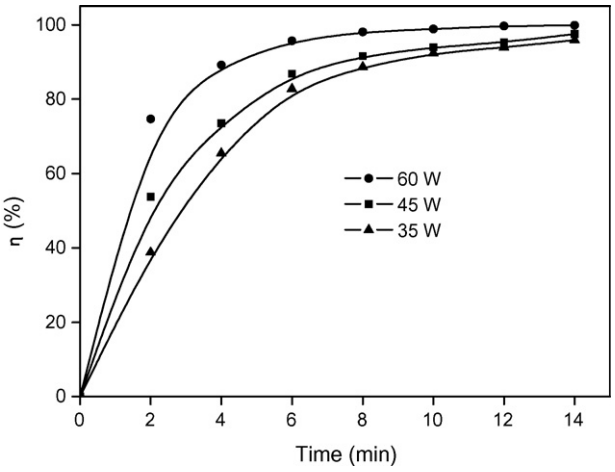

Fig. 2. Effect of output power intensity on the degradation efficiency of diuron (C_0 = 0.1 mmol L^{-1}, initial conductivity = 9.2 μS cm^{-1}, initial pH value = 6.20, air flow rate = 0.50 m^3 h^{-1}).

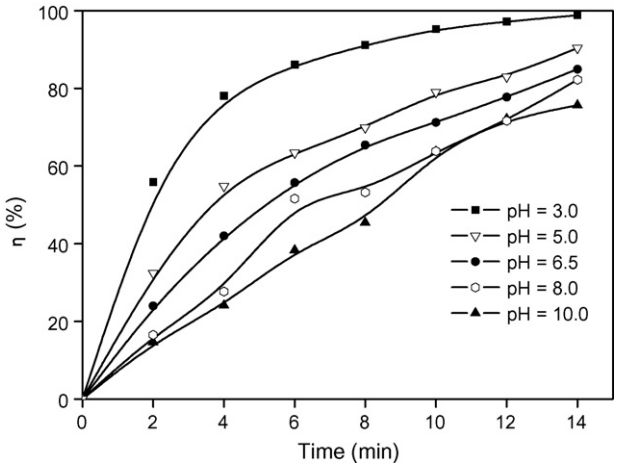

Fig. 3. Effect of pH value on the degradation efficiency of diuron (phosphate buffered) (C_0 = 0.1 mmol L^{-1}, initial conductivity = 440.0 μS cm^{-1}, output power intensity = 45 W, air flow rate = 0.50 m^3 h^{-1}).

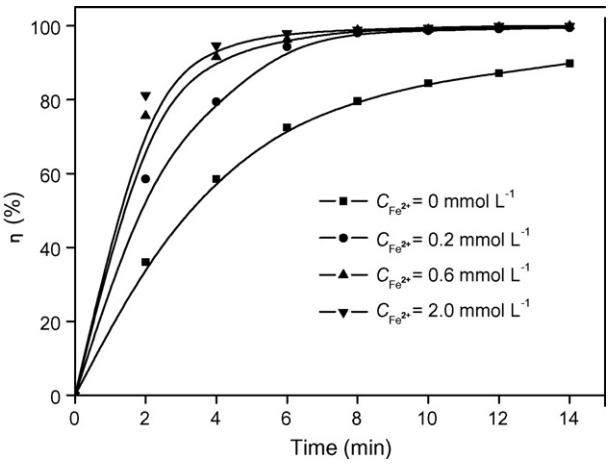

Fig. 4. Effect of Fe^{2+} concentration on the degradation efficiency of diuron (C_0 = 0.1 mmol L^{-1}, initial conductivity = 360.0 μS cm^{-1}, initial pH value = 6.20, output power intensity = 45 W, air flow rate = 0.50 m^3 h^{-1}).

ing equation (Eq. (2)):

$$\ln \frac{C_0}{C_t} = kt \quad (2)$$

where C_0, C_t and k were the initial concentration of diuron before discharge treatment (mmol L^{-1}), the residual concentration of diuron after discharge treatment (mmol L^{-1}) and the rate constant (min^{-1}), respectively. When $\ln(C_0/C_t)$ was plotted versus time, a good correlation was obtained for every set of data, which indicated that the degradation of diuron by gas–liquid hybrid discharge fitted first-order kinetics. The rate constant was 0.2448 min^{-1} in the case of 35 W. While in the case of 45 and 60 W, the rate constants were 0.2774 and 0.4785 min^{-1}, respectively.

3.1.2. Effect of pH value on the degradation efficiency of diuron

It is shown in Fig. 3 that the degradation efficiency of diuron was strongly affected by the pH value of the aqueous solution and was higher under acidic conditions. For example, the degradation efficiency of diuron reached 91.2% after 8 min of reaction time at pH value of 3.0, which was about two times greater than the degradation efficiency of diuron obtained at pH value of 10.0.

It was reported that the major active species, which were useful for the degradation of organic pollutants by pulsed discharge, were HO• and H_2O_2 [17]. And the direct HO• attack on many organic compounds was known to be strongly affected by pH. Under acidic conditions, more HO• radicals were produced and H_2O_2 decomposition was inhibited, thus the degradation efficiency of diuron was increased. While under alkaline conditions the generated HO• in the discharge reacted with carbonate ions immediately, which decreased the amount of HO• substantially [28]. Thus the degradation efficiency of diuron was decreased. The carbonate ions were derived from the breakdown of diuron and the degradation intermediates of diuron during the discharge process. It could be inferred from the above analyses that concentration of hydroxyl radicals is playing an important role in diuron degradation efficiency.

3.1.3. Effect of Fe^{2+} and Cu^{2+} on the degradation efficiency of diuron

In the previous work it was found that the presence of Fe^{2+} could improve the degradation efficiency of organic contaminants under the condition of pulsed discharge [29,30]. In the present work, degradation of diuron by gas–liquid hybrid discharge was conducted in the presence of Fe^{2+}. It is shown in Fig. 4 that the degradation efficiency of diuron increased dramatically in the presence of Fe^{2+} and also increased with increasing Fe^{2+} concentration under the same experimental conditions. The degradation efficiency of diuron was 58.5% after 4 min of reaction time in the absence of Fe^{2+}. While at the same discharge time, the degradation efficiencies of diuron were 79.4, 91.6 and 94.6% in the presence of Fe^{2+} at a concentration of 0.2, 0.6 and 2.0 mmol L^{-1}, respectively. The degradation efficiency enhancement in the presence of Fe^{2+} could be explained by the following equations [31–33]:

$$Fe^{2+} + H_2O_2 \rightarrow Fe(OH)^{2+} + HO^{\bullet} \quad (3)$$

$$Fe(OH)^{2+} + H_2O_2 \rightarrow Fe^{2+} + HO_2^{\bullet} + H_2O \quad (4)$$

$$Fe(OH)^{2+} \xrightarrow{h\nu} HO^{\bullet} + Fe^{2+} \quad (5)$$

In general, H_2O_2 was produced under the condition of gas–liquid hybrid discharge [17]. The oxidizing ability of the generated H_2O_2 was enhanced by the production of HO• from the classical Fenton reaction in the presence of Fe^{2+} [31]. At the same time, the degradation process was accelerated by the reduction of $Fe(OH)^{2+}$ species [34,35]. Therefore, the oxidation amount of diuron was increased.

pH value was one of the important parameters that influence the Fenton reaction. It has established that the optimum pH value for Fenton reaction was 2.8 [34,35]. While in the present work, the pH value of the solution decreased rapidly and kept around 2.8. The pH value of 2.8 was just the optimum pH value for Fenton reaction. Therefore further pH adjustment was not conducted in the presence of Fe^{2+}. Previous studies showed that higher Fe^{2+} concentration inhibited the degradation efficiency of organic substance because of the competition between Fe^{2+} and organic substance for HO•. The reaction was as follows [36]:

$$Fe^{2+} + HO^{\bullet} \rightarrow Fe^{3+} + OH^{-} \quad (6)$$

However, in the present study the inhibition effect was not observed.

Cu^{2+} also had the potential to react with H_2O_2 and produce HO•. It is shown in Fig. 5 that the adding of Cu^{2+} decreased the degradation efficiency of diuron during the first 4 min and increased the degradation efficiency of diuron during the last 10 min. Furthermore, the inhibition effect increased with increasing Cu^{2+} concentration and the stimulation effect also increased with increasing Cu^{2+} concentration. It was very clear that Fe^{2+} had better catalytic performance compared with Cu^{2+}. It is shown in Fig. 6 that the residual H_2O_2 concentration with Fe^{2+} or Cu^{2+} was lower

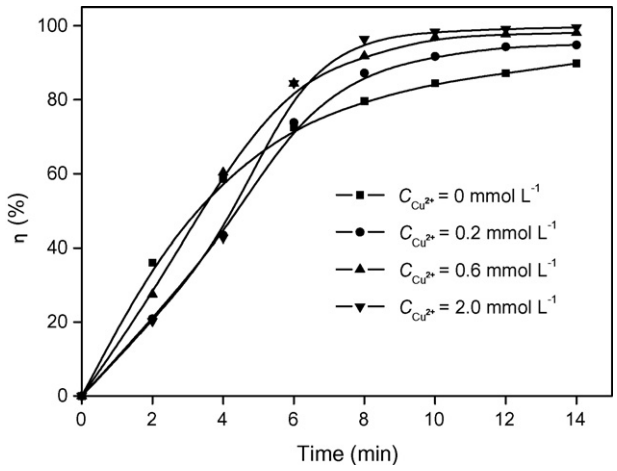

Fig. 5. Effect of Cu^{2+} concentration on the degradation efficiency of diuron (C_0 = 0.1 mmol L^{-1}, initial conductivity = 360.0 μS cm^{-1}, initial pH value = 6.20, output power intensity = 45 W, air flow rate = 0.50 m^3 h^{-1}).

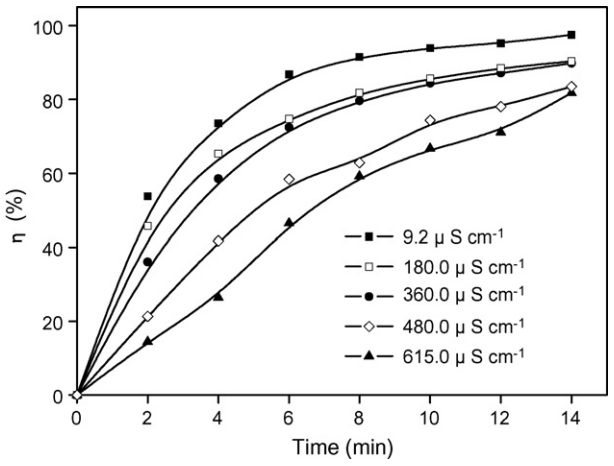

Fig. 7. Effect of initial conductivity on the degradation efficiency of diuron (C_0 = 0.1 mmol L^{-1}, initial pH value = 6.20, output power intensity = 45 W, air flow rate = 0.50 m^3 h^{-1}).

than that in the gas–liquid hybrid discharge process without metal ions. The lower concentration of residual H_2O_2 in the presence of Fe^{2+} was probably due to the consumption by Fe^{2+} and $Fe(OH)^{2+}$ (Eqs. (3) and (4)), which produced a larger amount of reactive radicals (HO• and HO_2•) and subsequently increased the degradation efficiency of diuron. While in the presence of Cu^{2+}, the produced H_2O_2 and Cu^{2+} were reacted to form $(Cu^{2+}OOH)^+$ octahedron complex (Eq. (7)), which decreased the concentration of residual H_2O_2 and subsequently decreased the degradation efficiency of diuron [37,38].

$$Cu^{2+} + H_2O_2 \rightarrow (Cu^{2+}OOH)^+ + H^+ \quad (7)$$

With increasing the discharge time, HO• was produced from the generated octahedron complex (Eq. (8)) [37,38]. Therefore, the degradation efficiency of diuron was increased.

$$(Cu^{2+}OOH)^+ \rightarrow Cu^+ + HO^\bullet + \tfrac{1}{2}O_2 \quad (8)$$

Furthermore, it is shown in Fig. 6 that the concentration of Fe^{2+} decreased with increasing reaction time. The reason might be that Fe^{2+} was oxidized to Fe^{3+} by the generated H_2O_2 and the introduced O_2 when air was bubbled into the reactor.

3.1.4. Effect of initial conductivity on the degradation efficiency of diuron

Conductivity was an important parameter that influences the discharge mode and radical intensity [39,40]. It is shown in Fig. 7 that the degradation efficiency of diuron decreased with increasing the conductivity under the same experimental conditions. The discharge mode changed from spark discharge to spark-streamer, and then the discharge mode changed from spark-streamer to corona discharge with increasing conductivity. At the same time, the conductivity of the diuron solution increased during the discharge process. The increase of liquid conductivity and change of discharge mode resulted in the slow diuron degradation trend after 10 min of reaction time, which was consistent with previous work [39,40].

3.1.5. Effect of air flow rate on the degradation efficiency of diuron

The air flow rate was one of the important parameters that affect the degradation efficiency of diuron. It is shown in Fig. 8 that the degradation efficiency of diuron increased with increasing the air flow rate from 0.05 to 0.50 m^3 h^{-1}. For example, the degradation efficiency of diuron reached 97.6% after 14 min of reaction time at an air flow rate of 0.50 m^3 h^{-1}, which was about two times greater than the degradation efficiency of diuron obtained at an air flow rate of

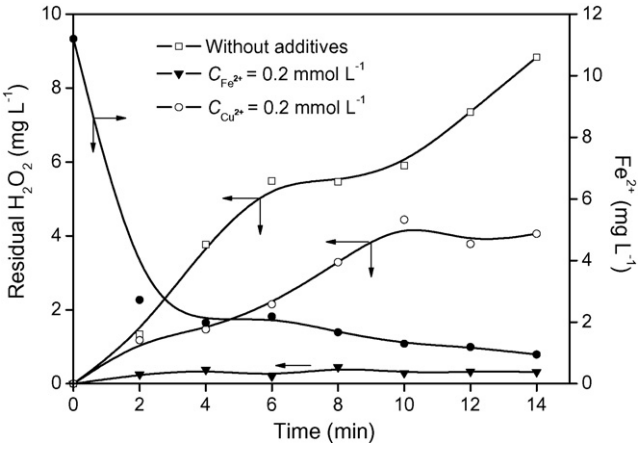

Fig. 6. Fe^{2+} and residual H_2O_2 concentrations during the reaction process (C_0 = 0.1 mmol L^{-1}, initial conductivity = 360.0 μS cm^{-1}, initial pH value = 6.20, output power intensity = 45 W, air flow rate = 0.50 m^3 h^{-1}).

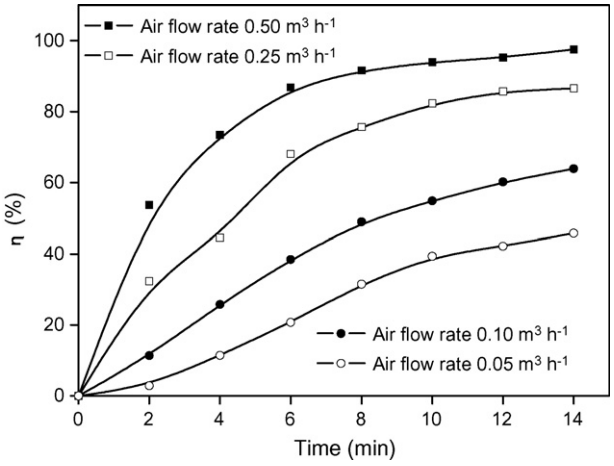

Fig. 8. Effect of air flow rate on the degradation efficiency of diuron (C_0 = 0.1 mmol L^{-1}, initial conductivity = 9.2 μS cm^{-1}, initial pH value = 6.20, output power intensity = 45 W).

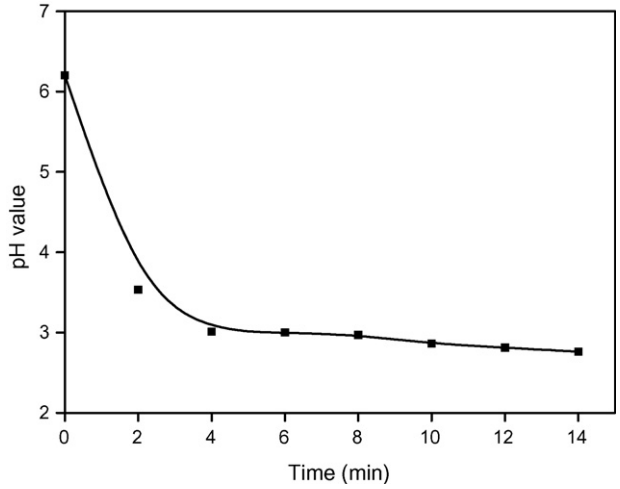

Fig. 9. Change of pH values during the reaction process (C_0 = 0.1 mmol L^{-1}, initial conductivity = 9.2 μS cm^{-1}, initial pH value = 6.20, output power intensity = 45 W, air flow rate = 0.50 m^3 h^{-1}).

0.05 m^3 h^{-1}. According to the bubble theory of liquid breakdown, when pulsed discharge took place with gas bubbling, there were more initial bubbles in solution near the sharp point, which accelerated electrons in the bubbles directly and resulted in an increase in the mean-free-path length of the electrons [41–43]. Therefore, higher speed energetic electrons could be obtained, as a result, the excitation and ionization of molecules occurred in the bubbles and solution, then more radicals (HO•, O•, H•) and molecular specials (H_2O_2, O_3) were produced. Furthermore, more radicals and molecular specials could be obtained when the air flow rate was increased, thus the degradation efficiency of diuron increased with increasing the air flow rate.

3.2. Change of pH values

It is shown in Fig. 9 that the pH value of the solution decreased rapidly during the first 4 min and then kept around 2.8 during the last 10 min. The decrease of the pH value might be due to the formation of H_3O^+, nitric acid and nitrous acid during discharge process [44]. Furthermore, the generated HCl because of the release of chlorine from diuron, and the formation of NH_4^+, NO_3^- and organic acids from diuron degradation should be responsible for the decrease of the pH value.

3.3. Removal of TOC

It is shown in Fig. 10 that the TOC removal rate increased in the presence of Fe^{2+} or Cu^{2+}. In the absence of Fe^{2+} and Cu^{2+}, the removal rate of TOC was only 22.4% within 14 min. While at the same discharge time the removal rate of TOC increased to 57.6 or 28.9% in the presence of Fe^{2+} or Cu^{2+} with the concentration of 0.6 mmol L^{-1}. It was well known that direct HO• production in gas–liquid hybrid discharge was much lower than the amount of HO• that could be produced from the hydrogen peroxide via the Fenton reaction. Therefore, the low mineralization rate of diuron in the absence of Fe^{2+} and Cu^{2+} might be due to the fact that lower quantity of HO• radicals were produced under the condition of gas–liquid hybrid discharge. Furthermore, diuron was probably degraded into other intermediates that were recalcitrant to be degraded. The enhancement of TOC removal rate in the presence of Fe^{2+} and Cu^{2+} could be attributed to the abundant amount of HO• generated by the above Eqs. (3), (5) and (8).

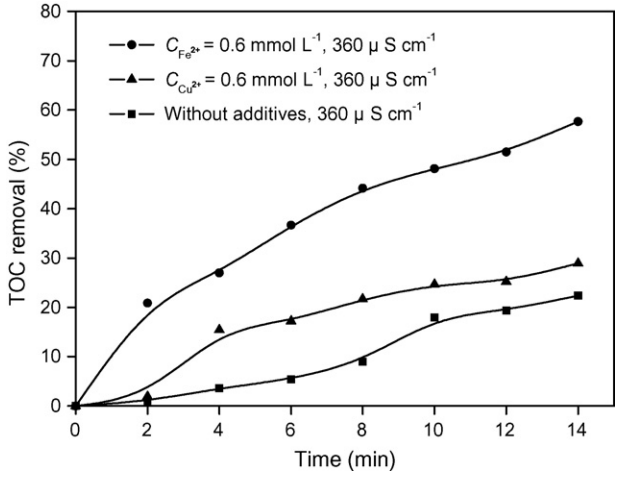

Fig. 10. Removal of TOC during the reaction process (C_0 = 0.1 mmol L^{-1}, initial pH value = 6.20, output power intensity = 45 W, air flow rate = 0.50 m^3 h^{-1}).

3.4. Formation of inorganic ions and organic acids

Inorganic ions such as Cl^-, NH_4^+ and NO_3^- were produced during the degradation process of diuron. The concentrations of Cl^-, NH_4^+ and NO_3^- in the gas–liquid hybrid discharge process were shown in Figs. 11 and 12, respectively. And the amount of the detected Cl^{-1} and Cl in the residual diuron after 14 min of reaction time was shown in Table 1. It is shown in Table 1 that the concentration of Cl^- was 4.63 mg L^{-1} in the absence of Fe^{2+} and Cu^{2+} after 14 min of reaction time. While in the presence of Cu^{2+} or Fe^{2+} with the concentration of 0.6 mmol L^{-1}, the concentration of Cl^- increased to 5.36 or 6.98 mg L^{-1} at the same reaction time. It was clear that the concentration of the detected Cl^- in the presence of Fe^{2+} with the concentration of 0.6 mmol L^{-1} was close to the stoichiometric value of Cl (7.1 mg L^{-1}). It is also shown in Table 1 that the sum of detected Cl^{-1} and Cl in the residual diuron with the adding of Cu^{2+} or without additives was lower than the stoichiometric value of Cl (7.1 mg L^{-1}) after 14 min of reaction time, which indicated that halogenated organic intermediates must be left in the solution. While the TOC removal rate was 57.6% within 14 min in the presence of Fe^{2+} with the concentration of 0.6 mmol L^{-1}, and the detected Cl^- amount approximated 100% of the total chlorine under the same experimental conditions, therefore, dechlorination occurred during the first steps of the reaction, and the nonhalo-

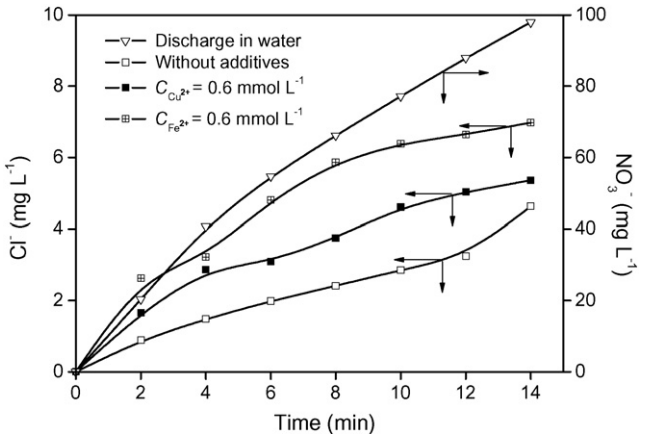

Fig. 11. Concentrations of Cl^- and NO_3^- during the reaction process (C_0 = 0.1 mmol L^{-1}, initial pH value = 6.20, output power intensity = 45 W, initial conductivity = 360.0 μS cm^{-1}, air flow rate = 0.50 m^3 h^{-1}).

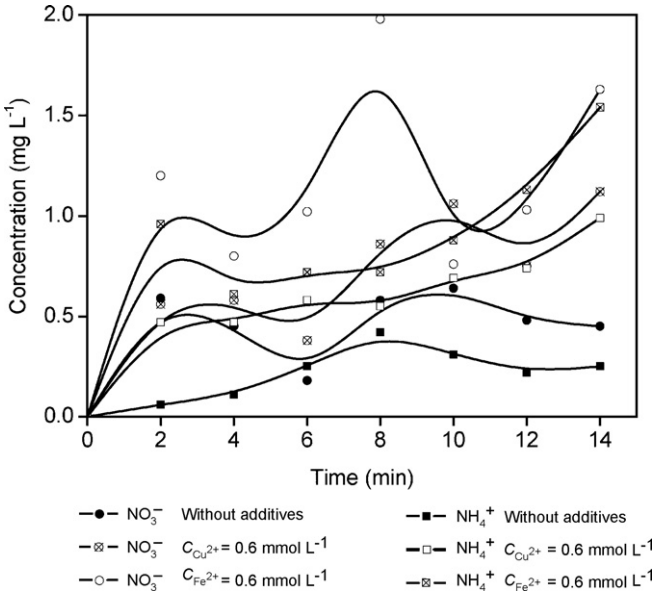

Fig. 12. Concentrations of NO_3^- and NH_4^+ during the reaction process (C_0 = 0.1 mmol L^{-1}, initial pH value = 6.20, output power intensity = 45 W, initial conductivity = 360.0 μS cm^{-1}, air flow rate = 0.50 m^3 h^{-1}).

genated organic intermediates were left in the solution. It is shown in Fig. 11 that the concentration of Cl^{-1} increased with increasing reaction time and also increased in the presence of Cu^{2+} or Fe^{2+}. It is also shown in Fig. 11 that large quantity of nitrate was formed from the air feed in the absence of diuron. The formation of nitrate from the nitrogen in the air must be responsible for the large drop in pH value (Fig. 9). It is shown in Fig. 12 and Table 1 that the concentrations of NH_4^+ and NO_3^- also increased in the presence of Cu^{2+} or Fe^{2+}. While the stoichiometric value of N was 2.8 mg L^{-1} (0.1 mmol L^{-1} diuron), therefore, only small amount of the total N was detected as NH_4^+ and NO_3^- after 14 min of reaction time. Thus other nitrogen-containing compounds must exist in the solution or evaporate during the process.

The concentrations of acetic acid, formic acid and oxalic acid during the reaction process were shown in Fig. 13. The amount of organic acid as C, TOC and C in the residual diuron after 14 min of reaction time was shown in Table 1. It is shown in Fig. 13 that acetic acid, formic acid and oxalic acid all existed after 14 min of reaction time. It was noticeable that the amounts of organic acids formed in the presence of Fe^{2+} were all greater than those without additives. It is shown in Table 1 that the sum of organic acids as C, TOC and C

Table 1
Detected Cl^{-1}, Cl in the residual diuron, NH_4^+ and NO_3^- as N, N in the residual diuron, organic acids as C, TOC and C in the residual diuron after 14 min of reaction time (C_0 = 0.1 mmol L^{-1}, initial pH value = 6.20, output power intensity = 45 W, initial conductivity = 360.0 μS cm^{-1}, air flow rate = 0.50 m^3 h^{-1})

Items	Without additives	$C_{Cu^{2+}}$ = 0.6 mmol L^{-1}	$C_{Fe^{2+}}$ = 0.6 mmol L^{-1}
(A) Detected Cl^{-1} (mg L^{-1})	4.63	5.36	6.98
(B) Cl in the residual diuron (mg L^{-1})	0.72	0.13	0.01
(A) + (B) (mg L^{-1})	5.35	5.49	6.99
(C) NH_4^+ and NO_3^- as N (mg L^{-1})	0.29	1.02	1.57
(D) N in the residual diuron (mg L^{-1})	0.29	0.05	0.003
(C) + (D) (mg L^{-1})	0.58	1.07	1.57
(E) Organic acids as C (mg L^{-1})	0.48	0.87	1.94
(F) TOC (mg L^{-1})	9.20	8.79	5.24
(G) C in the residual diuron (mg L^{-1})	1.10	0.21	0.01
(E) + (F) + (G) (mg L^{-1})	10.78	9.87	7.19

Table 2
Retention time, structures of diuron and degradation products

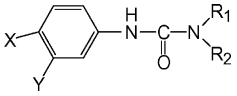

Compound	m/z	Retention time (min)	X	Y	R_1	R_2
1	111	7.56	–	–	–	–
2 (Diuron)	231	8.06	Cl	Cl	CH_3	CH_3
3	245	12.66	Cl	Cl	CH_3	CHO
4	247	11.95	Cl	Cl	CH_3	CH_2OH
5	249	11.84	Cl	Cl	H	$CH(OH)_2$
6	261	7.95	Cl	Cl	CH_3	COOH
7	263	7.75	Cl	Cl	CH_3	$CH(OH)_2$
8	277	5.68	Cl	Cl	CH_2OH	COOH
9	278	5.30	–	–	–	–
10	292	5.19	–	–	–	–

in the residual diuron with the adding of Fe^{2+} was lower than that with the adding of Cu^{2+} or without additives. The generated acetic acid could be attributed to the opening of the aromatic ring [45]. The direct oxidation of methyl groups, oxalic acid and acetic acid resulted in the formation of formic acid [46]. Moreover, formic acid, oxalic acid and acetic acid also appeared as the degradation products during the degradation process of diuron by other methods [45,47].

3.5. The proposed degradation pathway

The identification of diuron and its degradation intermediates was performed by extensive LC–MS. The same method has been successfully used for the identification of diuron degradation intermediates by other researchers [45,47]. In some cases, the intermediates detected in the present work were compared with those obtained previously [45,47–49].

By interpreting the mass spectra, 9 degradation products of diuron were detected. The retention time and structures of the degradation products were listed in Table 2. In addition to these intermediates, other degradation products, such as the non-halogenated organic intermediates, could exist in the solution. Nevertheless, they were not detected because of the employed chromatography column and the low concentrations of these intermediates. Malato et al. and Tahmasseb et al. also detected compound **3** during the degradation process of diuron by solar photocatalysis and ozonation, respectively [45,48]. Compounds **3**, **4**, **5** and **7** were also detected as the intermediates under the condition of photo-Fenton treatment of diuron [47]. Shankar et al. also detected compounds **3** and **4** [49]. Compounds **6** and **8** were the newly reported molecules. Based on the detected Cl^{-1} and the intermediate products found in this work, the proposed degradation pathway of diuron by gas–liquid hybrid discharge was proposed in Scheme 1. It could be inferred that the attack on the aromatic ring and the methyl group of diuron by the generated active species resulted in the formation of various intermediates. Evolution of the intermediates during the reaction process was shown in Fig. 14.

Various active species such as radicals (HO•, O•, H•) and molecular specials (H_2O_2, O_3) were generated in gas–liquid hybrid discharge process [16,17]. Among these radicals and molecular specials, HO• was an electron deficient group, which had strong electrophilic property and high redox potential, thus the reaction between HO• and aromatic ring compounds might not obey general orientation rules [50]. The generation mechanism of various intermediates could be interpreted as follows: degradation of diuron in the gas–liquid hybrid discharge reactor was ignited by the generated HO•. HO• reacted with one methyl group on the aliphatic side chain of diuron by an abstraction of hydrogen atom, as a result,

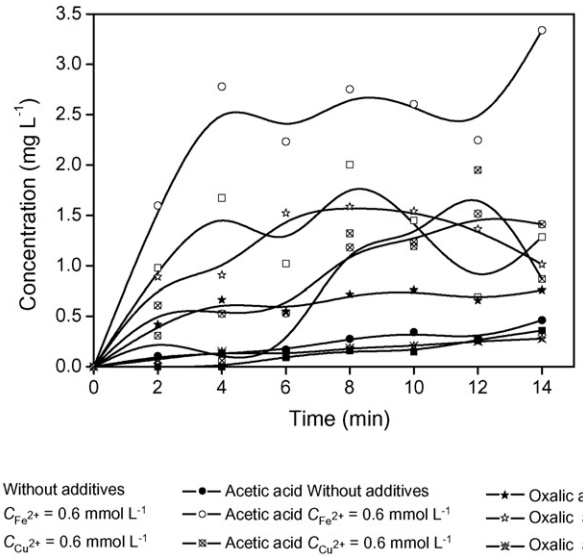

Fig. 13. Concentrations of acetic acid, formic acid and oxalic acid during the reaction process (C_0 = 0.1 mmol L^{-1}, initial pH value = 6.20, output power intensity = 45 W, initial conductivity = 360.0 μS cm^{-1}, air flow rate = 0.50 m^3 h^{-1}).

a radical ($R_1^{\bullet}$) was produced. In the solution, the radical ($R_1^{\bullet}$) reacted with oxygen preferentially and yielded a peroxyl radical ($R_1OO^{\bullet}$). Owing to its disproportionation, passing probably through a tetraoxide transient, two degradation products compounds **3** and **4** were formed [9]. Compound **7** was identified as the product formed by the attack of $HO^{\bullet}$ to the methyl group of compound **4** [47]. In addition, compounds **3** and **6** were identified as the oxidation products of compound **7**. Compound **5** was suggested as the product formed by the attack of $OH^{\bullet}$ to the second methyl group of diuron once the first methyl group was eliminated. This demethylation process had been proposed previously and occurred through the formation of hydroxylated or carboxylated compounds as follows [51,45]:

$$\text{R-CH}_3 \rightarrow \text{R-CH}_2\text{OH and/or R-CHO and/or R-COOH} \rightarrow \text{R-H}$$

The formation mechanism of compound **8** was similar to that of compound **4**. Opening of the aromatic ring was realized by the for-

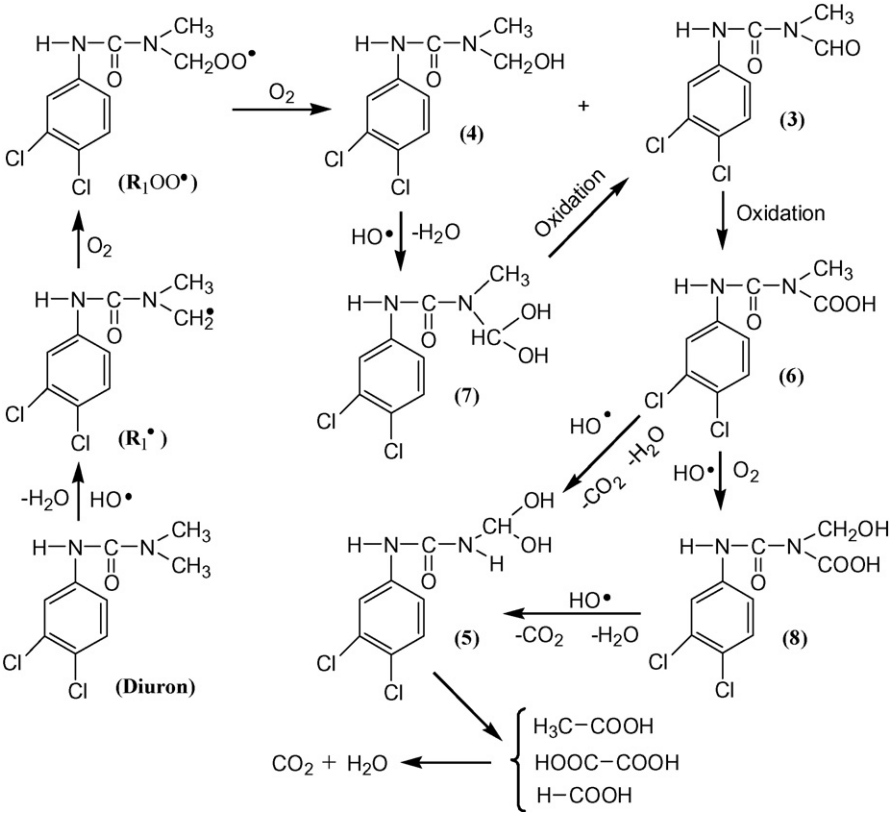

Scheme 1. The proposed degradation pathway of diuron.

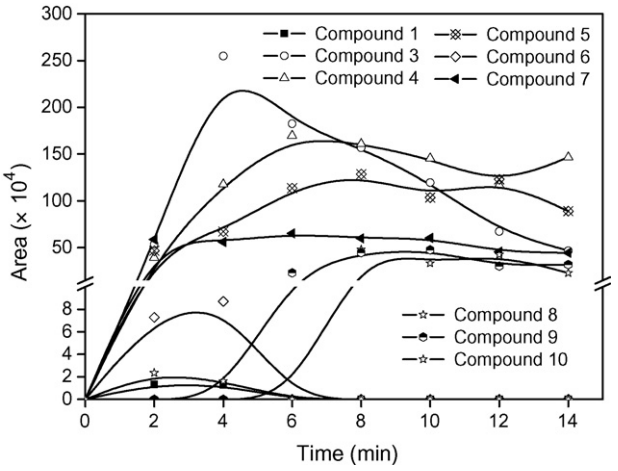

Fig. 14. Evolution of the intermediates during the reaction process (C_0 = 0.1 mmol L^{-1}, initial pH value = 6.20, output power intensity = 45 W, initial conductivity = 9.2 μS cm^{-1}, air flow rate = 0.50 m^3 h^{-1}).

mation of organic acids [45]. Finally, mineralization was realized by producing H_2O and CO_2 as the final products.

4. Conclusions

The degradation efficiency of diuron increased with increasing output power intensity. The degradation of diuron by gas–liquid hybrid discharge fitted first-order kinetics. The degradation efficiency of diuron increased with decreasing pH value. The presence of Fe^{2+} increased the degradation efficiency of diuron and the degradation efficiency of diuron increased with increasing Fe^{2+} concentration. Cu^{2+} addition decreased the degradation efficiency of diuron during the first 4 min and increased the degradation efficiency of diuron during the last 10 min. Furthermore, during the first 4 min the inhibition effect increased with increasing Cu^{2+} concentration and the stimulation effect also increased with increasing Cu^{2+} concentration during the last 10 min. Decreasing the initial conductivity and increasing the air flow rate were favorable for the degradation of diuron. The pH value of the solution decreased rapidly during the first 4 min and then kept around 2.8 during the last 10 min. The generated Cl^-, NH_4^+, NO_3^-, acetic acid, formic acid and oxalic acid were detected in the present work. Based on the detected intermediate products, the proposed degradation pathway of diuron by gas–liquid hybrid discharge was proposed. The aromatic ring and the methyl group of diuron were the main sites that were usually attacked by the active species.

Acknowledgements

The authors thank the Natural Science Foundation of China (No. 10475040) and Shanghai Tongji Gao Tingyao Environmental Science & Technology Development Foundation (China) for financial support. We would like to thank Wenming Yan and Zhaobing Guo for their help in the experimental work.

References

[1] S. Giacomazzi, N. Cochet, Environmental impact of diuron transformation: a review, Chemosphere 56 (2004) 1021–1032.
[2] S. Chiron, A. Fernandez-Alba, A. Rodriguez, E. Garcia-calvo, Pesticide chemical oxidation: state-of-the-art, Water Res. 34 (2000) 366–377.
[3] H. Okamura, I. Aoyama, Y. Ono, T. Nishida, Antifouling herbicides in the coastal waters of western Japan, Mar. Pollut. Bull. 47 (2003) 59–67.
[4] M.H. Lamoree, C.P. Swart, A. van der Horst, B. van Hattum, Determination of diuron and the antifouling paint biocide Irgarol 1051 in Dutch marinas and coastal waters, J. Chromatogr. A 970 (2002) 183–190.
[5] Pesticides 2002, A Summary of Monitoring the Aquatic Environment in England and Wales, Environment Agency, Bristol, UK, 2002.
[6] M.I.M. Rubio, W. Gernjak, I.O. Alberola, J.B. Galvez, P. Fernandez-Ibanez, S.M. Rodriguez, Photo-Fenton degradation of alachlor, atrazine, chlorfenvinphos, diuron, isoproturon and pentachlorophenol at solar pilot plant, Int. J. Environ. Pollut. 27 (2006) 135–146.
[7] A.M. Polcaro, M. Mascia, S. Palmas, A. Vacca, Electrochemical degradation of diuron and dichloroaniline at BDD electrode, Electrochim. Acta 49 (2004) 649–656.
[8] K. Macounova, J. Klima, C. Bernard, C. Degrand, Ultrasound-assisted anodic oxidation of diuron, J. Electroanal. Chem. 457 (1998) 141–147.
[9] K. Macounová, H. Krýsová, J. Ludvík, J. Jirkovský, Kinetics of photocatalytic degradation of diuron in aqueous colloidal solutions of Q-TiO_2 particles, J. Photochem. Photobiol. A 156 (2003) 273–282.
[10] M.J. Farré, X. Domènech, J. Peral, Assessment of photo-Fenton and biological treatment coupling for diuron and linuron removal from water, Water Res. 40 (2006) 2533–2540.
[11] M.L. Canle, S. Rodríguez, L.F. Rodríguez Vázquez, J.A. Santaballa, S. Steenken, First stages of photodegradation of the urea herbicides fenuron, monuron and diuron, J. Mol. Struct. 565–566 (2001) 133–139.
[12] M. El Madani, C. Guillard, N. Pérol, J.M. Chovelon, M. El Azzouzi, Photocatalytic degradation of diuron in aqueous solution in presence of two industrial titania catalysts, either as suspended powders or deposited on flexible industrial photoresistant papers, Appl. Catal. B: Environ. 65 (2006) 70–76.
[13] H. Okamura, Photodegradation of the antifouling compounds Irgarol 1051 and Diuron released from a commercial antifouling paint, Chemosphere 48 (2002) 43–50.
[14] M.J. Farré, M.I. Franch, S. Malato, J.A. Ayllón, J. Peral, X. Doménech, Degradation of some biorecalcitrant pesticides by homogeneous and heterogeneous photocatalytic ozonation, Chemosphere 58 (2005) 1127–1133.
[15] L.C. Lei, Y. Zhang, X.W. Zhang, Y.J. Shen, Using a novel pulsed high-voltage gas–liquid hybrid discharge continuous reactor for removal of organic pollutant in oxygen atmosphere, J. Electrostat. 66 (2008) 16–24.
[16] B. Sun, M. Sato, J.S. Clements, Oxidative processes occurring when pulsed high voltage discharges degrade phenol in aqueous solution, Environ. Sci. Technol. 34 (2000) 509–513.
[17] A.A. Joshi, B.R. Locke, P. Arce, W.C. Finney, Formation of hydroxyl radicals, hydrogen peroxide and aqueous electrons by pulsed streamer corona discharge in aqueous solution, J. Hazard. Mater. 41 (1995) 3–30.
[18] B. Sun, M. Sato, J.S. Clements, Use of a pulsed high-voltage discharge for removal of organic compounds in aqueous solution, J. Phys. D: Appl. Phys. 32 (1999) 1908–1915.
[19] M. Sato, T. Ohgiyama, J.S. Clements, Formation of chemical species and their effects on microorganisms using a pulsed high-voltage discharge in water, IEEE Trans. Ind. Appl. 32 (1996) 106–112.
[20] M. Sahni, B.R. Locke, The effects of reaction conditions on liquid-phase hydroxyl radical production in gas–liquid pulsed-electrical-discharge reactors, Plasma Process. Polym. 3 (2006) 668–681.
[21] M. Sahni, B.R. Locke, Quantification of hydroxyl radicals produced in aqueous phase pulsed electrical discharge reactors, Ind. Eng. Chem. Res. 45 (2006) 5819–5825.
[22] P. Sunka, V. Babický, M. Clupek, P. Lukes, M. Simek, J. Schmidt, M. Cernák, Generation of chemically active species by electrical discharges in water, Plasma Sources Sci. Technol. 8 (1999) 258–265.
[23] Y. Zhang, M.H. Zhou, X.L. Hao, L.C. Lei, Degradation mechanisms of 4-chlorophenol in a novel gas–liquid hybrid discharge reactor by pulsed high voltage system with oxygen or nitrogen bubbling, Chemosphere 67 (2007) 702–711.
[24] J. Xue, L. Chen, H.L. Wang, Degradation mechanism of Alizarin Red in hybrid gas–liquid phase dielectric barrier discharge plasmas: experimental and theoretical examination, Chem. Eng. J. 138 (2008) 120–127.
[25] H. Kušić, N. Koprivanac, B.R. Locke, Decomposition of phenol by hybrid gas/liquid electrical discharge reactors with zeolite catalysts, J. Hazard. Mater. B 125 (2005) 190–200.
[26] State Environmental Protection Administration of China, Water and Wastewater Analytical Method, fourth ed., China Environmental Sciences Press, Beijing, 2002.
[27] C. Kormann, D.W. Bahnemann, M.R. Hoffmann, Photocatalytic production of H_2O_2 and organic peroxides in aqueous suspensions of TiO_2, ZnO, and desert sand, Environ. Sci. Technol. 22 (1988) 798–806.
[28] A.T. Sugiarto, S. Ito, T. Ohshima, M. Sato, J.D. Skalny, Oxidative decoloration of dyes by pulsed discharge plasma in water, J. Electrostat. 58 (2003) 135–145.
[29] X.L. Hao, M.H. Zhou, Q. Xin, L.C. Lei, Pulsed discharge plasma induced Fenton-like reactions for the enhancement of the degradation of 4-chlorophenol in water, Chemosphere 66 (2007) 2185–2192.
[30] D.R. Grymonpré, A.K. Sharma, W.C. Finney, B.R. Locke, The role of Fenton's reaction in aqueous phase pulsed streamer corona reactors, Chem. Eng. J. 82 (2001) 189–207.
[31] C. Walling, Fenton's reagent revisited, Acc. Chem. Res. 8 (1975) 125–131.
[32] R. Buvet, P. Sechaud, J. Darolles, L. Le Port, F. Sechaud, Electrochemical and chemical reductions of oxygen dissolved in aqueous solutions, Bioelectrochem. Bioenergy 18 (1987) 13–19.

[33] E. Neyens, J. Baeyens, A review of classic Fenton's peroxidation as an advanced oxidation technique, J. Hazard. Mater. B 98 (2003) 33–50.
[34] J.J. Pignatello, Dark and photoassisted Fe^{3+}-catalyzed degradation of chlorophenoxy herbicides by hydrogen peroxide, Environ. Sci. Technol. 26 (1992) 944–951.
[35] Y.F. Sun, J.J. Pignatello, Photochemical reactions involved in the total mineralization of 2,4-D by Fe^{3+}/H_2O_2/UV, Environ. Sci. Technol. 27 (1993) 304–310.
[36] A.M. Wang, J.H. Qu, J. Ru, H.J. Liu, J.T. Ge, Mineralization of an azo dye Acid Red 14 by electro-Fenton's reagent using an activated carbon fiber cathode, Dyes Pigments 65 (2005) 227–233.
[37] C.H. Wei, C.S. Hu, B. Yang, C.F. Wu, Efficacy of homogenous catalyst for wet oxidation of formaldehyde-containing wastewater, Environ. Chem. 22 (2003) 459–463 (in Chinese).
[38] L.A. Kaplan, D.J. Reasoner, E.W. Rice, A survey of BOM in U.S. drinking waters, J. Am. Water Works Assoc. 86 (1994) 121–132.
[39] L.C. Lei, Y. Zhang, X.W. Zhang, Y.X. Du, Q.Z. Dai, S. Han, Degradation performance of 4-chlorophenol as a typical organic pollutant by a pulsed high voltage discharge system, Ind. Eng. Chem. Res. 46 (2007) 5469–5477.
[40] B. Sun, M. Sato, J.S. Clements, Optical study of active species produced by a pulsed streamer corona discharge in water, J. Electrost. 39 (1997) 189–202.
[41] J.S. Clements, M. Sato, R.H. Davis, Preliminary investigation of prebreakdown phenomena and chemical reactions using a pulsed high-voltage discharge in water, IEEE Trans. Ind. Appl. 23 (1987) 224–235.
[42] B. Sun, M. Sato, A. Harano, J.S. Clements, Non-uniform pulse discharge-induced radical production in distilled water, J. Electrostat. 43 (1998) 115–126.
[43] Y.S. Chen, X.S. Zhang, Y.C. Dai, W.K. Yuan, Pulsed high-voltage discharge plasma for degradation of phenol in aqueous solution, Sep. Purif. Technol. 34 (2004) 5–12.
[44] Y.S. Mok, S.W. Ham, I.S. Nam, Mathematical analysis of positive pulsed corona discharge process employed for removal of nitrogen oxides, IEEE Trans. Plasma Sci. 26 (1998) 1566–1574.
[45] S. Malato, J. Cáceres, A.R. Fernández-Alba, L. Piedra, M.D. Hernando, A. Agüera, J. Vial, Photocatalytic treatment of diuron by solar photocatalysis: evaluation of main intermediates and toxicity, Environ. Sci. Technol. 37 (2003) 2516–2524.
[46] M.I. Franch, J.A. Ayllón, J. Peral, X. Domènech, Photocatalytic degradation of short-chain organic diacids, Catal. Today 76 (2002) 221–233.
[47] M.J. Farré, S. Brosillon, X. Doménech, J. Peral, Evaluation of the intermediates generated during the degradation of diuron and linuron herbicides by the photo-Fenton reaction, J. Photochem. Photobiol. A 189 (2007) 364–373.
[48] L.A. Tahmasseb, S. Nélieu, L. Kerhoas, J. Einhorn, Ozonation of chlorophenylurea pesticides in water: reaction monitoring and degradation pathways, Sci. Total Environ. 291 (2002) 33–44.
[49] M.V. Shankar, S. Nélieu, L. Kerhoas, J. Einhorn, Photo-induced degradation of diuron in aqueous solution by nitrites and nitrates: kinetics and pathways, Chemosphere 66 (2007) 767–774.
[50] J.M. Shen, Z.L. Chen, Z.Z. Xu, X.Y. Li, B.B. Xu, F. Qi, Kinetics and mechanism of degradation of *p*-chloronitrobenzene in water by ozonation, J. Hazard. Mater. 152 (2008) 1325–1331.
[51] L. Lhomme, S. Brosillon, D. Wolbert, J. Dussaud, Photocatalytic degradation of a phenylurea, chlortoluron, in water using an industrial titanium dioxide coated media, Appl. Catal. B: Environ. 61 (2005) 227–235.